3

The Paleocene-Eocene Thermal Maximum: Feedbacks Between Climate Change and Biogeochemical Cycles

Arne Max Erich Winguth
University of Texas at Arlington
USA

1. Introduction

It is predicted that by the year 2300, the atmospheric CO_2 concentration will exceed ~2000 ppmv (Caldeira & Wickett, 2003; Mikolajewicz et al., 2007), corresponding to a release of 4000 x 10^{15} g carbon (PgC) by fossil fuel emissions and land use changes since the beginning of the industrial revolution. The anthropogenic carbon will eventually sequester on time scales of 100,000 yrs as organic carbon into the ocean and land biosphere and as $CaCO_3$ into the geosphere (Archer et al., 1998). This carbon transfer in the atmosphere-ocean system is comparable to that at the Paleocene-Eocene boundary (55 Ma), when a massive release of carbon into the climate system led to a prominent global warming event referred to as the Paleocene-Eocene Thermal Maximum (PETM). The PETM is characterized by a major (>3.0‰) negative carbon isotope excursion, documented in marine and terrestrial fossils (e.g. Koch et al., 1992; Kelly et al., 1998; Handley et al., 2008), and a worldwide seafloor carbonate dissolution horizon (e.g. Bralower et al., 1997; Lu et al., 1998; Schmitz et al., 1996; E. Thomas et al., 2000) as well as shoaling of the lysocline and carbonate compensation depth (Zachos et al., 2005). These changes are consistent with the release of more than 2000 PgC of isotopically depleted carbon into the ocean-atmosphere system within less than 10,000 years (Panchuk et al., 2008; Zachos et al., 2007, 2008), pointing to a greenhouse gas-driven warming (see Fig. 1). Recent estimates from Cui et al. (2011) indicate a slow emission rate of 0.3-1.7 PgC yr^{-1} as compared to the present-day emission of carbon dioxide of ~9.9 PgC yr^{-1} from fossil fuel emissions (Boden et al., 2010) and land-use changes (Houghton, 2008). Surface temperatures increased by 5°C in the tropics (Tripati & Elderfield, 2005; Zachos et al., 2005) and mid-latitudes (Wing et al., 2005), and by 6-8°C in the ice-free Arctic and sub-Antarctic (Hollis et al., 2009; Kennett & Stott, 1991; Moran et al., 2006; Sluijs et al., 2006, 2007, 2008a, 2011; E. Thomas et al., 2000; Weijers et al., 2007), and deep-sea temperatures increased by 4-6°C (Tripati and Elderfield, 2005; Zachos et al., 2008), relative to Paleocene temperatures (see Fig. 1). At the same time, large-scale changes in the climate system occurred, for example in the patterns of atmospheric circulation, vapor transport, precipitation (Robert & Kennett, 1994; Pagani et al., 2006a; Brinkhuis et al., 2006; Sluijs et al., 2008a, 2011; Wing et al., 2005), intermediate and deep-sea circulation (Nunes & Norris 2006; D.J. Thomas, 2004; D.J. Thomas et al., 2008) and a rise in global sea level (Sluijs et al., 2008b; Handley et al., 2011). The sea level rise is caused by various factors, including thermal

expansion, decrease in ocean basin volume, decrease in mountain glaciers, as well as local tectonic changes. Topography and bathymetry during the PETM differed significantly from today with respect to the distribution of landmasses, sizes of ocean basins and width and depth of seaways.

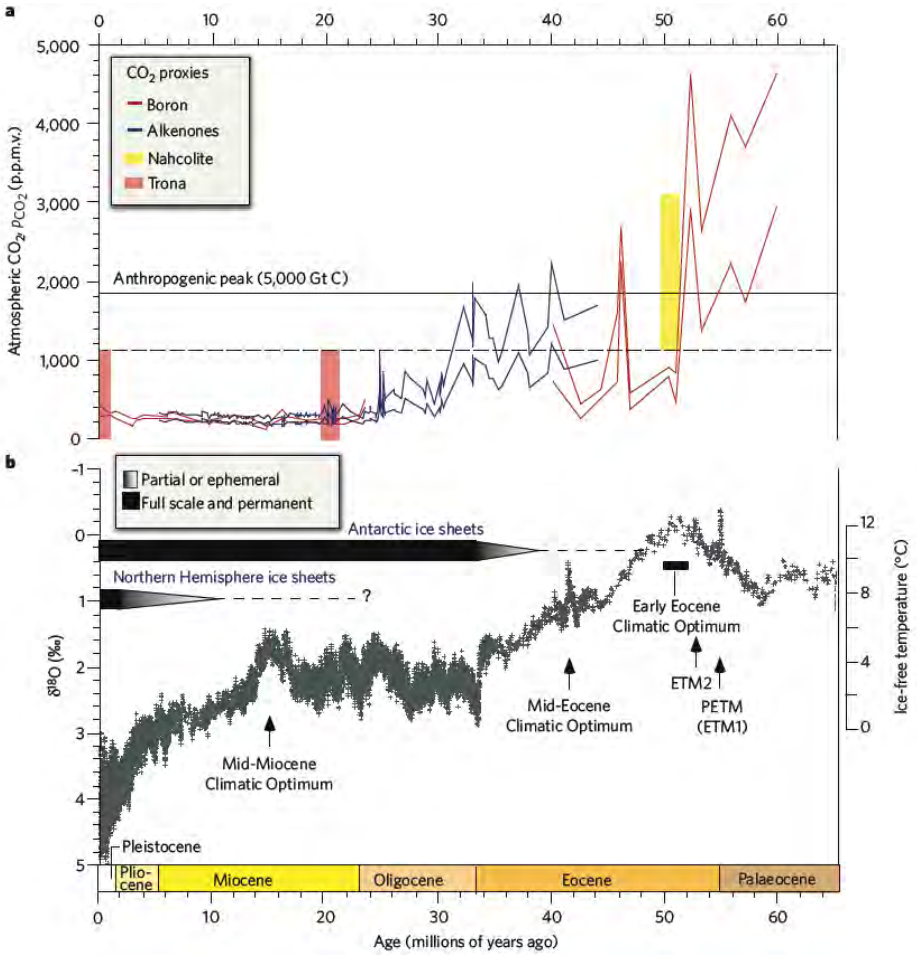

Fig. 1. Evolution of atmospheric pCO_2 concentration and deep-sea temperature reconstruction over the past 65 million years (from Zachos et al., 2008). a) Atmospheric pCO_2 for the period 0 to 65 million years ago. The dashed horizontal line shows the minimum pCO_2 for the early Eocene (1,125 ppmv), as given by calculations of equilibrium with Na–CO_3 mineral phases (vertical bars, where the length of the bars indicates the range of pCO_2 over which the mineral phases are stable) that are found in Neogene and early Eocene lacustrine deposits. The vertical distance between the upper and lower colored lines shows the range of uncertainty for the alkenone and boron proxies. b) Deep-sea benthic foraminiferal oxygen-isotope curve based on records from Deep Sea Drilling Project and Ocean Drilling Program sites. [Reproduced by permission of AAAS; copyright 2008 AAAS.]

2. Climate change and variability at the beginning of the PETM

The causes leading to the warming event at the Paleocene-Eocene boundary are still controversial (Fig. 2).

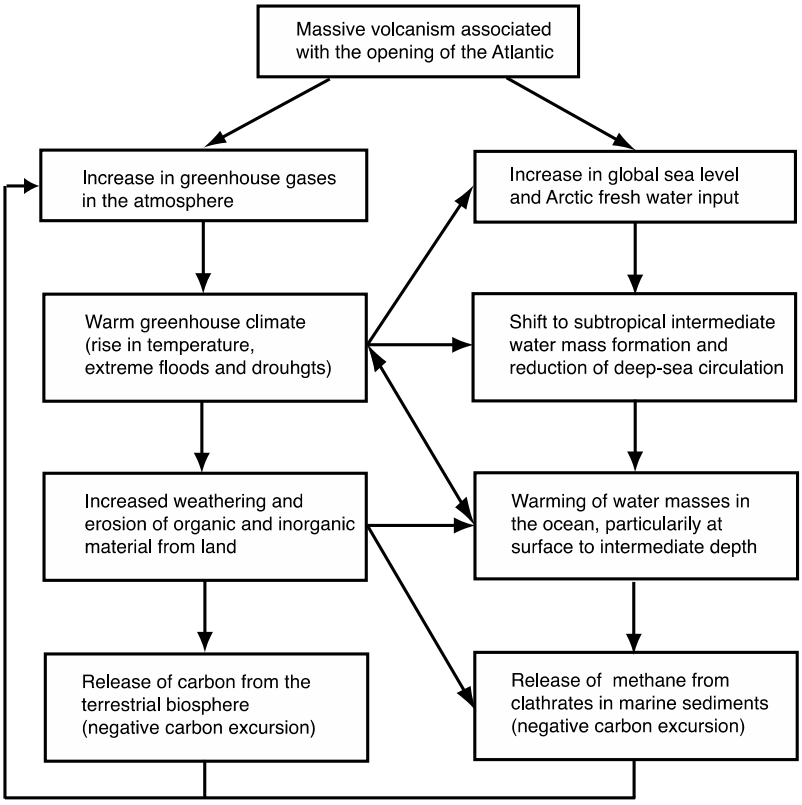

Fig. 2. Major feedbacks for the initial warming at the Paleocene-Eocene boundary. Note that the feedbacks and their magnitudes are still controversial (see e.g. Bowen and Zachos, 2010).

One possible sequence of events inferred from paleoproxies begins with a volcanically induced greenhouse gas (water vapor, CO_2, CH_4, and other constituents) increase that would have produced a global increase in surface temperature (Bralower et al., 1997; Kennett & Stott, 1999; Sluijs et al., 2007, 2011; E. Thomas et al., 2000). Various climate-modeling studies have investigated the warming event at the Paleocene-Eocene boundary in response of the elevated greenhouse gas concentrations. These studies utilized atmospheric general circulation models (Sloan & Barron, 1992; Sloan & Rea, 1995; Huber & Sloan, 1999; Shellito et al., 2003; Shellito & Sloan, 2006), ocean general circulation models (Bice et al., 2000; Bice & Marotzke, 2002), or more recently coupled comprehensive climate models (Heinemann et al., 2009; Huber & Sloan, 2001; Huber & Caballero, 2003; Huber & Caballero, 2011; Lunt et al., 2010; Shellito et al., 2009; Winguth et al., 2010) to simulate the mean climate

and its variability during the Eocene, but they have not been able to reproduce the high temperatures of the PETM in the high latitudes, and were controversial regarding the cause of this warming (Pagani et al., 2006b; Zeebe et al., 2009).
Some of the more recent studies have investigated the climate feedbacks with a sequence of different greenhouse gas concentrations (e.g. Heinemann et al., 2009; Lunt et al., 2010; Winguth et al., 2010). In the following, we summarize key findings of the paper of Winguth et al. (2010), using a complex earth system model, the comprehensive Community Climate System Model version 3 (CCSM-3; Collins et al., 2006), in order to investigate PETM climate feedbacks in response to rises in the greenhouse gas concentrations. Huber & Caballero (2011) used the same model, but with a different dust concentration in the atmosphere. The simulated increase by 2.5°C from $4xCO_2$ to $8xCO_2$ in CCSM-3 could be explained by CO_2 emissions due to enhanced volcanic activity at the beginning of the PETM (Fig. 3).

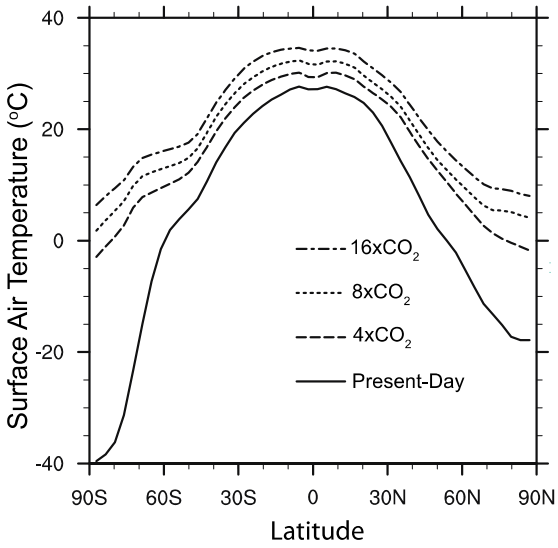

Fig. 3. Zonally averaged (50-yr mean) surface air temperature (in °C) for present-day (solid), $4xCO_2$ PETM (long-dashed), $8xCO_2$ PETM (short-dashed), and $16xCO_2$ PETM (dashed-dotted)(from Winguth et al., 2010).

Surface temperatures in the tropics rise by only ~2°C from $4xCO_2$ to $8xCO_2$, in agreement with temperature reconstructions (Pearson et al., 2007) and with future climate predictions (IPCC, 2007) of a more extreme warming at high latitudes vs. low latitudes in a warmer world. Temperature increase over land exceeds that over the ocean (Fig. 4) due to reduced latent heat fluxes and lower heat capacity. Over the continents, the 30°C isotherm in the $8xCO_2$ simulation reaches up to 30° latitude, about 5° more poleward than for the present-day simulation. Maximum simulated temperatures, comparable to extreme temperatures in the present-day Sahara, are simulated over subtropical Africa and South America (~50°C for $8xCO_2$), resulting in warm sea-surface temperatures in the adjacent oceans through advection. Simulated minimum surface temperatures (for $8xCO_2$) are between 3°C and 7°C over the Arctic and about -10°C over northeast Asia.

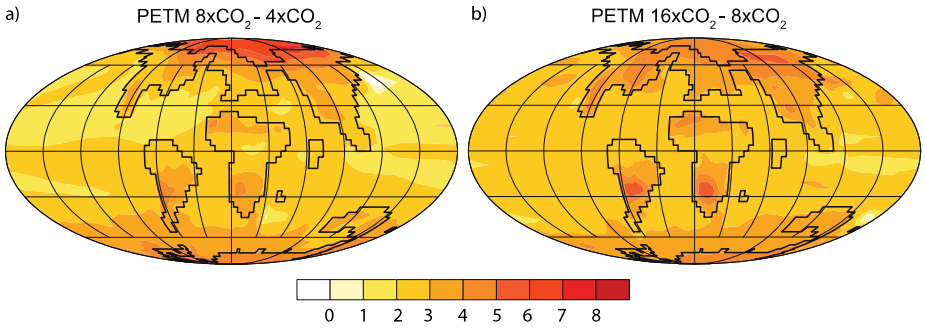

Fig. 4. Surface air temperature (SAT) in °C for a) the difference between the 8x and the 4xCO_2 PETM experiment corresponding to opening of the Atlantic by massive volcanism and b) differences between the 16x and the 8xCO_2 PETM experiment by the release of carbon from the marine and terrestrial carbon stocks (100-year mean).

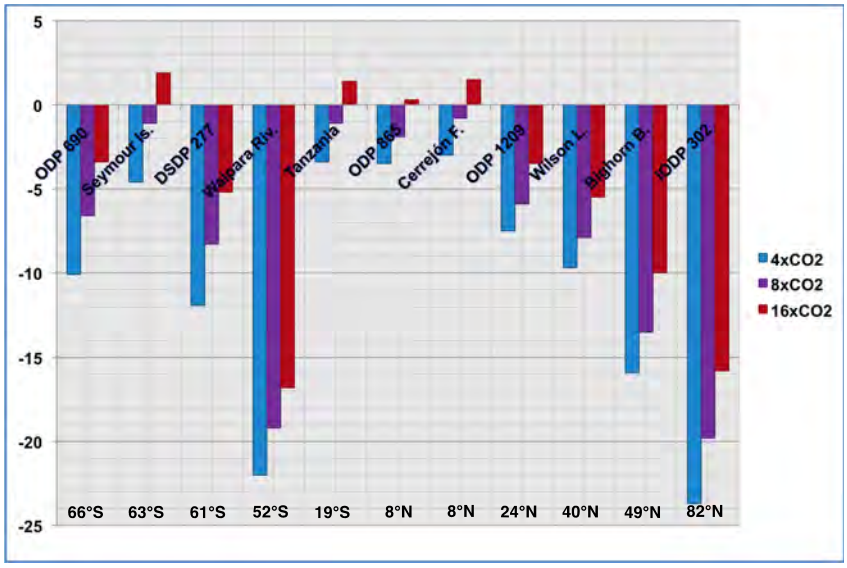

Fig. 5. Differences between reconstructed surface temperatures (in °C) and 50-year annual mean temperature from the CCSM-3 climate simulation with an atmospheric CO_2 concentration of 4x (blue), 8x (purple), and 16x (red) the preindustrial level (see Winguth et al., 2010). For reference, paleolatitude is listed for each location.

While data-inferred paleotemperatures are relatively well represented in the tropical regions, a significant bias between model results and data remains for the Arctic Ocean (Sluijs et al., 2006) and for the area around New Zealand (Fig. 5, Waipara River; Hollis et al., 2009). The bias in the northern polar region (IODP core 302 A; Sluijs et al., 2006) is of complex nature and could for example be associated with the concentration of cloud

condensation nuclei used in CCSM-3 (Huber & Caballero, 2011; Kump & Pollard, 2008), the uncertainties in paleolocations (N-S position, or distance form shore), or with skewing of data towards summer temperatures (Sluijs et al., 2006). The causes for model-data discrepancies at high southern latitudes remain controversial.

A positive climate-carbon cycle feedback loop leading to further PETM warming due to destabilization of methane hydrates is shown in Fig. 2. There is sufficient evidence from various sites around the globe, including the New Jersey shelf (Sluijs et al., 2007), the North Sea (Bujak & Brinkhuis, 1998; Sluijs et al., 2007), the Southern Ocean (Kennett and Stott, 1991), and New Zealand (Hollis et al., 2009) that ^{13}C-depleted carbon in the form of isotopically light CO_2 and/or CH_4 was released from the sea floor (Dickens et al., 1995, 1997; Higgins & Schrag, 2006; Pagani et al., 2006a) or from wetlands (Pancost et al., 2007) into the atmosphere-ocean-biosphere system (Sluijs et al., 2007; Bowen and Zachos, 2010). As shown in Figs. 3 and 4, such a change in the radiative forcing from $8xCO_2$ to $16xCO_2$ leads to a simulated additional warming of ~2°C globally, with 4°C at the poles, 5°C over South America and South Africa, and 2°C at the equator. For the Southern Ocean, cool water masses moderate the climate over the polar southern hemisphere, so that south of 60°, the temperature increase in response to the increase of CO_2-radiative forcing is smaller than in the northern hemisphere (Fig. 4b). In mid-latitudes, the bias between the $16xCO_2$ simulation and reconstructed PETM surface temperatures is reduced compared to simulations with a lower atmospheric CO_2 level with high dust concentration; the values are comparable to the $8xCO_2$ scenario with lower dust concentration in Huber & Caballero (2011). For the tropics, evidence from fossil remains of a giant boid snake in northeastern Colombia (Head et al., 2009) and modeling studies (Winguth et al., 2010; Huber & Caballero, 2011) support warm average temperatures of 30-34°C.

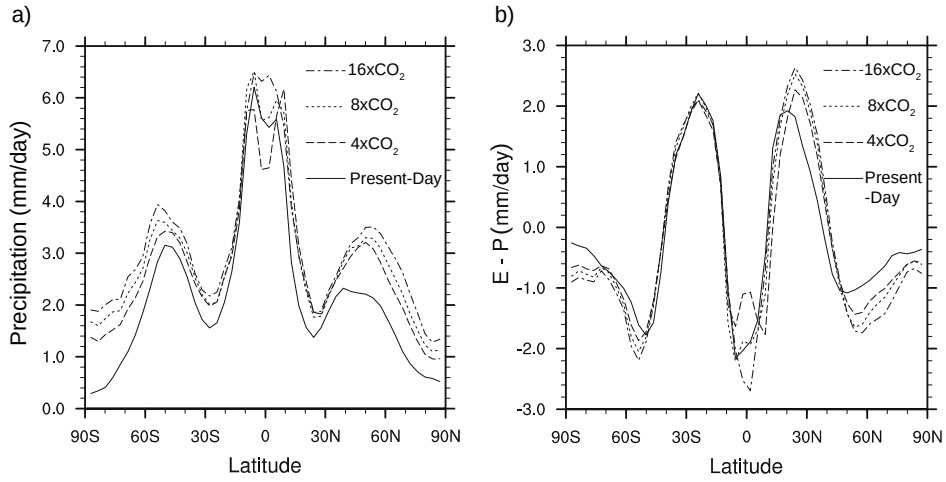

Fig. 6. Zonally averaged (50-yr mean) precipitation (in mm/day) (a) and evaporation minus precipitation (in mm/day) (b) for present-day (solid), $4xCO_2$ PETM (long-dashed), $8xCO_2$ PETM (short-dashed), and $16xCO_2$ PETM (dashed-dotted) (from Winguth et al., 2010). The increase in global warming during the PETM leads to extremes in the hydrological cycle (droughts in the subtropics and higher precipitation and flooding in the tropics and high latitudes).

Rapid warming at the beginning of the Eocene has been inferred from the widespread distribution of dinoflagellate cysts (or dynocysts). The abundance of one dynocyst species, Apectodinium, dramatically increased at different locations worldwide (Bujak & Brinkhuis, 1998; Crouch et al., 2001; Heilmann-Clausen & Egger, 2000; Sluijs et al., 2007), implying a change in environmental conditions such as warmer sea surface temperatures and increased food availability in form of phytoplankton (Burkholder et al., 1992) due to increased nutrient delivery by weathering (Ravizza et al., 2001; Zachos & Dickens, 2000) and erosion (Fig. 2).
The climate-carbon cycle feedback associated with an increase in greenhouse gases (Fig. 2) might also have been enhanced by an increase in the atmospheric water vapor fluxes (Figs. 6 and 7); for instance, latent heat flux by evaporation and precipitation rises with the warming of the surface (Fig. 6). Higher precipitation and lower sea surface salinity values are derived for the Arctic from isotopic measurements as well as from dinocyst assemblages (Pagani et al., 2006a; Sluijs et al., 2008a). The enhanced precipitation at high latitudes is consistent to patterns simulated for future climate scenarios (e.g. Cubasch et al., 2001; Meehl et al., 2006; Mikolajewicz et al., 2007). For the southern high latitudes, a simulated increase in precipitation is confirmed by clay-mineral indicators from the Antarctic continent, pointing towards humid conditions at the PETM (Robert & Kennett, 1994). Compared to present-day, differences in the geography and mountain height cause remarkable changes. For instance, a higher than present-day ratio of tropical land-to-ocean area at the PETM reduces the tropical ocean surface and hence the oceanic source of atmospheric moisture (Barron et al., 1989). This change in tropical surface area not only reduces significantly tropical precipitation, but also poleward moisture transport from the tropics. However, increase in precipitation by higher than present-day greenhouse gases counteracted this effect during the PETM.

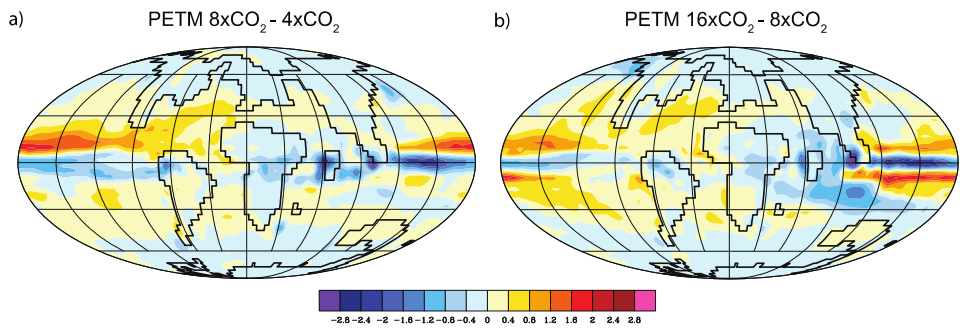

Fig. 7. Evaporation minus precipitation (in mm/day) for a) the difference between the 8x and the 4xCO_2 PETM experiment, and b) the difference between the 16x and the 8xCO_2 PETM simulation. The increase in global warming during the PETM leads to extremes in the hydrological cycle (increases in aridity in the subtropics are shaded red, and in humidity in the tropics are shaded blue).

An initial increase in CO_2 in the atmosphere by volcanic outgassing would have increased the strength of the hydrological cycle. Model simulations suggest that the subtropics at ~30° became drier and that precipitation at 60° increased significantly (Fig. 6), which is consistent to future climate projections (IPCC, 2007). Over North America during summer, the

simulated total amount of rainfall decreases from lower to mid-latitudes in response to a northward-directed monsoonal moisture transport over the Mississippi watershed from the Gulf (Sewall & Sloan, 2006; Winguth et al., 2010). Sedimentary records from the mid-latitudes of the North American continent have produced conflicting evidence for hydrological changes in this region. For example, a ~25% increase in relative humidity for the northern continental mid-latitudes (Bighorn Basin, Wyoming, paleolatitude ~49 °N) has been inferred from an amplification in the carbon isotope excursion in soil organic matter (Bowen et al., 2004), but vegetation analysis inferred a decrease of ~40% in precipitation at the beginning of the PETM (Wing et al., 2005). Drier PETM conditions occurred probably in Utah (USA, paleolatitude ~45 °N; Bowen & Bowen, 2008); these findings are, however, controversial, since other studies (Retallack, 2005) suggest enhanced rainfall for this region (Bowen & Bowen, 2009; Retallack, 2009). Droughts by reduced soil moisture and biomass burning through wildfires in the subtropics during the PETM could have provided a significant carbon release to the atmosphere (Fig. 7).
In western Europe, sedimentary records from the Spanish Pyrenees (Schmitz & Pujalte, 2007) indicate seasonally increased precipitation during the PETM, leading to enhanced runoff into the Tethys Ocean and thus enhanced productivity by a rise in nutrient availability in the near-shore areas (Schmitz et al., 1996; Speijer & Wagner, 2002; Gavrilov et al., 2003). Increased precipitation over England (~+1 mm/day change from $4xCO_2$ to $16xCO_2$) would also have generated a feedback on the carbon cycle, for example enhanced carbon emission from wetlands (Pancost et al., 2007).

3. Feedbacks associated with the PETM ocean circulation

In this section, two feedback loops involving the carbon cycle and climate are discussed. The first is associated with the rise of greenhouse gas concentrations (water vapor, CO_2, CH_4, and other gases) in the atmosphere due to tectonic changes such as volcanism (Bralower et al., 1997; Kennett & Stott, 1991; Lyle et al., 2008; Sluijs et al., 2007; Storey et al., 2007; Svensen et al., 2004) and the second with the response of the climate system to regional or global sea level change by tectonic uplift and climatic changes (Fig. 2). Evidence of marine transgression during the PETM (Handley et al., 2011; Maclennan & Jones, 2006; Schmitz & Pujalte, 2003; Sluijs et al., 2008b) related to changes in spreading rate, volcanism, and regional perturbations as well as climatic changes (melting of glaciers, thermal expansion, and changes in ocean circulation) suggests that sea levels rose by approximately 20-30 m. The increase in surface temperatures and freshening of the sea surface by enhanced poleward moisture transport in response to a rise of greenhouse gases changes the regional buoyancy and momentum fluxes, leading to changes in vertical density gradients and stratification of the deep sea. Warmer and more saline subtropical water masses are modeled associated with the initial PETM warming (~0.2 psu higher in salinity for the $8xCO_2$ than for the $4xCO_2$ experiment), originating near the Gulf of Mexico and mixed via the eastern North Atlantic into intermediate layers. For intermediate water masses in the North Atlantic Ocean, simulated temperature rises by ~4°C (from ~11°C to ~15°C) (Fig. 8a).
In the Pacific, the increase of the atmospheric CO_2 to $8xCO_2$ results in an increase in the vertical density gradient, since surface waters become significantly lighter with the warming. Deep-sea temperatures increase by ~2.5°C due to the global warming (Fig. 8b). The simulated Pacific circulation in the $4xCO_2$ scenario is nearly symmetric about the equator, with deep-sea ventilation occurring in the polar regions of the northern and

southern hemisphere (Fig. 9a), in agreement with analyses of Nd isotope data that indicated a bimodal ventilation (D.J. Thomas et al., 2008). The northward-directed Atlantic deep-sea circulation of ~4 Sv (1 Sv = 10^6 m^3 s^{-1}) in the 4xCO_2 scenario with a source of deep-water formation in the South Atlantic is comparable in strength with the modern but reversed.
With an increase of the CO_2-radiative forcing to 8xCO_2, the ventilation of the deep sea is reduced and the age of water masses in intermediate depth is increased (Fig. 9b), particularly in the southern high latitudes. The Atlantic deep-sea circulation in the 8xCO_2 scenario remains reversed, in agreement with Zeebe & Zachos (2007), who used inferred [CO_3^{2-}] gradients in the deep sea, but in contrast with the reconstruction of an abrupt shift in the deep-sea circulation during the PETM to a North Atlantic deep-water source, based on benthic carbon isotope records (Nunes & Norris, 2006).

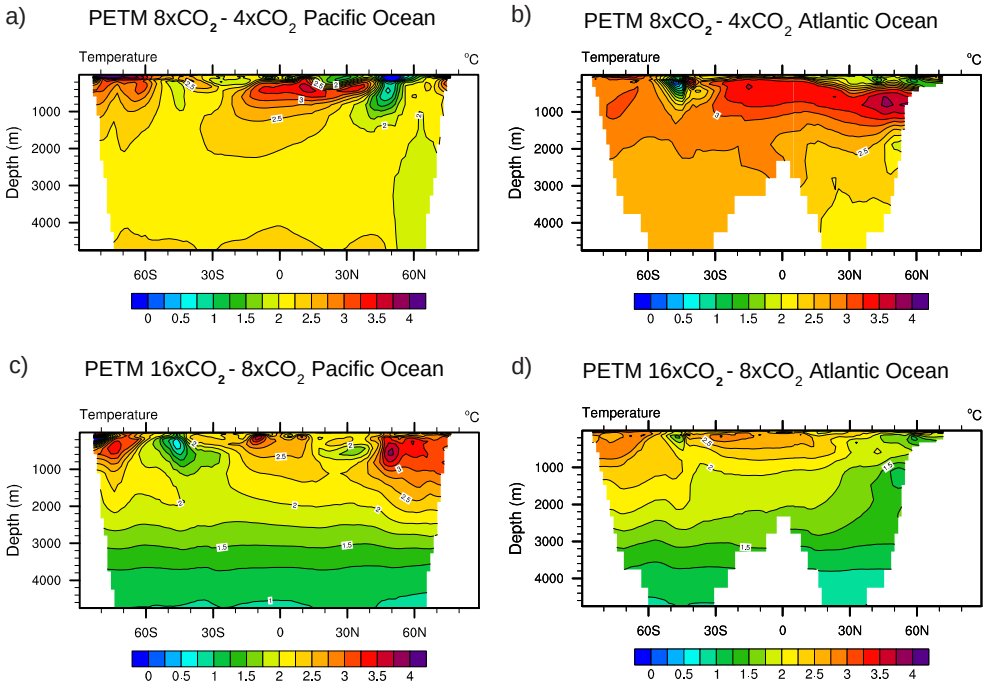

Fig. 8. Vertical sections of the potential temperature (50-year mean) differences of the 8xCO_2 and 4xCO_2 PETM experiments for the Pacific Ocean (a) and the Atlantic Ocean (b) for the beginning of the warming, and differences of the 16xCO_2 and the 8xCO_2 PETM experiments for the Pacific Ocean (c) and the Atlantic Ocean (d) (from Winguth et al., 2010).

The warming of intermediate and deep-water masses could have had a positive feedback on the ocean circulation (Fig. 2), as proposed in Bice & Marotzke (2002). The warming of the ocean by changes in the buoyancy forcing (heat and freshwater fluxes) and circulation lowers the depth of methane hydrate stability, which depends on pressure, temperature, salinity, and gas composition, from ~900 m to ~1500 m (Fig. 10; Dickens et al., 1995). This change might have triggered a massive methane hydrate release into the atmosphere-ocean

system, which in turn accelerated the global warming (Archer & Buffett, 2005). The potential consequences of such an amplification are displayed in Figs. 8c and d, for the assumption that the carbon release corresponded to ~4400 PgC ($16xCO_2$ experiment) relative to the $8xCO_2$ experiment. A temperature increase of >3.5°C is simulated for high-latitude intermediate water masses in the Pacific due to an increase in vertical density gradients. The increase in the ideal age of water masses is shown in Fig. 9c.

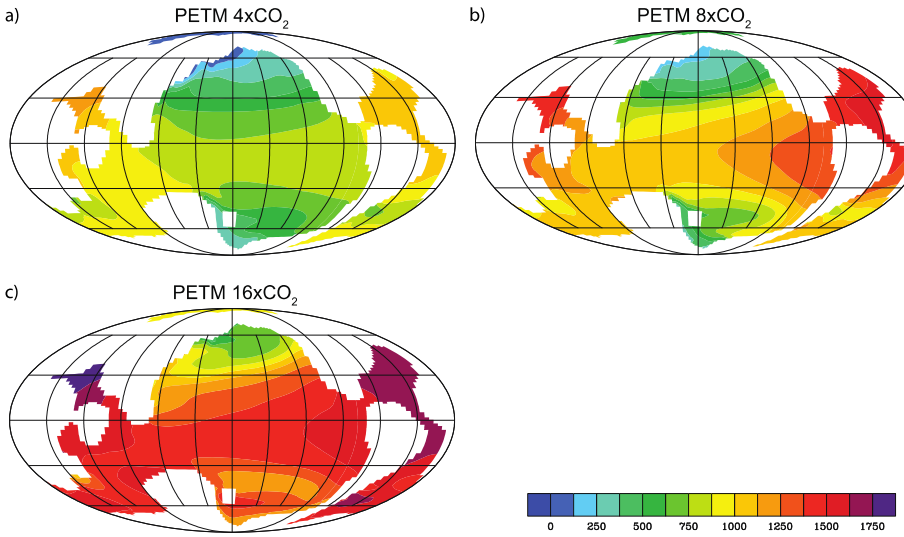

Fig. 9. Change of residence time of water masses in ~1800 m depth (idealized age in yrs) for a) $4xCO_2$ PETM simulation, b) $8xCO_2$ PETM simulation, and c) $16xCO_2$ PETM simulation (100-yr mean). Increase of idealized age corresponds to an increase in stratification. Locations of deep-sea ventilation are in the Northern and Southern Pacific. The deep-sea ventilation decreases particularly in the southern ocean with higher atmospheric CO_2 radiative forcing.

The feedback loop associated with the sea level changes at the PETM would have affected the oceans by an enhanced freshing from Arctic Ocean. An increased flow via the Turgay Strait, the passage between the Arctic and Tethys Ocean, has been inferred from the abundance of dinoflagellate cysts (e.g. Iakokleva et al., 2001). Higher sea levels might also have allowed a throughflow via the Fram and Bering Straits, as supported by Nd-Sr isotopes in fish fossils (Gleason et al., 2009; Roberts et al., 2009), paleogeographic reconstructions (Scotese, 2011) and climate simulations (Cope & Winguth, 2011; Heinemann et al., 2009).
A freshwater input from the Arctic Ocean into the North Pacific Ocean (Marincovich & Gladenkov, 1999) would have produced an increase in the vertical density gradients and led to a weakening of the North Pacific intermediate water masses by 2.5 Sv at 30°N, and a comparable increase in the Pacific deep-sea circulation. The opening of the Bering Strait would have shifted formation of intermediate water masses in the North Pacific more equatorward towards the arid subtropics, by that increasing temperature and salinity of intermediate water masses (Fig. 11). Such a temperature change in intermediate waters at

the beginning of the PETM warming could have contributed to the release of methane hydrates (e.g. Kennett & Stott, 1991; Sluijs et al., 2007). Most of the methane released from the hydrates would have ultimately reached the atmosphere or oxidized as CO_2 and thus increased the greenhouse gas radiative forcing during the PETM (Fig. 2).

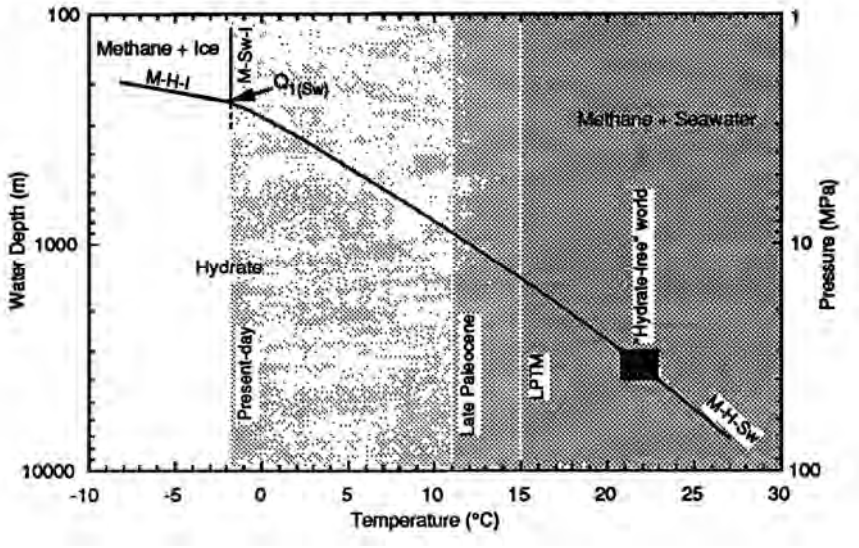

Fig. 10. Methane-hydrate temperature-depth (pressure) diagram from Dickens et al. (1995), adapted after Dickens & Quinby-Hunt (1994). The triple point (Q_1) is the point where all three phases (methane and sea ice, methane and sea water, methane hydrates) meet. Above the triple point to the left are conditions where methane and sea ice and to the right where methane and seawater exist. The area below the curve denotes the conditions under which methane hydrates are stable (at present-day with bottom water temperatures of -1.5 °C and depths below 250 m). For the pre-PETM, the critical depth below which methane hydrates were stable was around 900 m. A 4°C water temperature increase at the PETM would have lowered the critical depth by ~600 m to ~1500 m. [Reproduced by permission of American Geophysical Union; copyright 1995 American Geophysical Union.]

4. Feedbacks associated with the atmospheric chemistry during the PETM

Many potentially important feedback processes are associated with atmospheric chemistry (Beerling et al., 2007).

Possible changes associated with clouds at the beginning of the PETM are for example cloud albedo, cloud optical depth, or heat transport by tropical cyclones. Clouds interfere with the transfer of radiation because they reflect a certain amount of radiation back to space and they act as a blanket for thermal radiation. The reflectivity of clouds is influenced by cloud condensation nuclei (CCN). While today's major source for CCN over land is due to pollution, CCN concentrations over remote ocean areas are linked to marine productivity via dimethyl sulfide (DMS) emission from the ocean. DMS emitted from certain phytoplankton groups is mixed into the troposphere and is oxidized to sulfate particles,

which then act as CCN for marine clouds. The CCN concentration affects cloud droplet size and distribution, which influences cloud reflectivity and hence the climate. Climate change on the large scale, in turn, affects the ocean circulation, nutrient cycles and consequently the phytoplankton concentration in the oceans and thereby closes via DMS emission the feedback loop, as first hypothesized by Charlson et al. (1987). If global productivity had declined during the PETM by ocean stagnation and reduced equatorial upwelling, the concentration of CCN would also have been reduced.

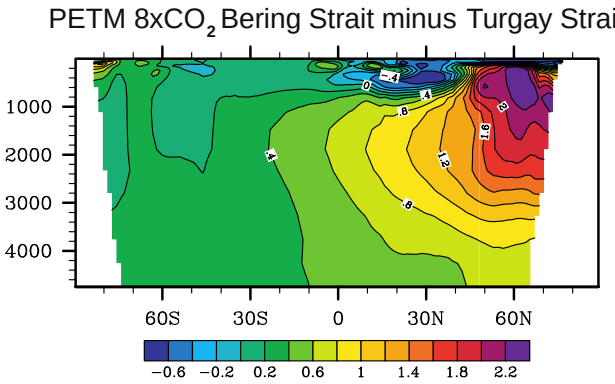

Fig. 11. Vertical section of the potential temperature (50-year mean) difference of the 8xCO_2 PETM simulation with a passage between the Arctic Ocean and the Pacific (Bering Strait) minus the simulation with a passage between the Arctic Ocean and the Indian Ocean. The changes in throughflow might have been caused by sea level rise due to tectonic and climatic changes (Fig. 2). A change of freshwater input from the Arctic might ultimately have caused warming of water masses and thus triggered a positive feedback loop between the climate and the carbon cycle.

This would have affected the cloud optical depth (Kump and Pollard, 2008), leading to high-latitude warming and a further increase in ocean stratification and stagnation of the deep-sea circulation, probably similar to the one modeled in the 16xCO_2 experiment by Winguth et al. (2010). Polar stratospheric clouds (Sloan & Pollard, 1998; Kirk-Davidoff et al., 2002) or intensified tropical cyclone activity (Korty et al., 2008) could have further exaggerated warming at the PETM.

Another feedback between the carbon cycle and the climate that may have played an important role during the PETM are volatile organic compounds (VOCs; Beerling et al., 2007). VOCs are emitted by plants, for example isoprene with present-day emission rates comparable to that of methane (Guenther et al., 2006; Prather & Erhalt, 2001). Isoprene is a major player in the oxidative chemistry of the troposphere and influences the formation of tropospheric ozone (Fehsenfeld et al., 1992), decreases the hydroxyl radical concentration, increases the residence time of CH_4, and is involved in forming organic aerosols influencing the climate by acting as CCN (Beerling et al., 2007).

High CH_4 emissions during the PETM could have increased the atmospheric methane concentration and enhanced radiative forcing (with a ~21 times higher global warming potential than CO_2 over a time span of 100 years; IPCC, 1990). Methane in the atmosphere is typically either reduced by oxidation to CO_2 or interacts with other chemical components.

Emission scenarios for the PETM considering atmospheric chemistry involving NOx and ozone reactions indicate that the life-time of methane in the atmosphere increases with increasing emission of methane, thus leading to an increased radiative forcing influencing the climate and methane hydrate destabilization within a positive feedback loop (Schmidt & Shindell, 2003).

5. Feedbacks associated with weathering during the PETM

While the feedbacks listed in the previous sections illustrate the complexity of the PETM warming, the rapid recovery phase after the CIE remains controversial as well. Rapidly regrowing organic carbon stocks on land and in the ocean on climatic time scales $<10^4$ years may have contributed to a draw-down of the atmospheric CO_2 concentration (Bowen & Zachos, 2010), thus creating a positive feedback between a cooler climate and a more vigorous ocean circulation with reduced vertical density gradients and enhanced ventilation from high latitudes (Fig. 12). Intensification of wind-driven upwelling and enhanced high-latitude mixing stimulate global productivity through higher nutrient availability in the euphotic zone. Such an increase in the productivity (Bains et al., 1999; Stoll et al., 2007; Sluijs et al., 2006) could eventually have accelerated the draw-down of the atmospheric CO_2.
On longer geologic timescales ($>10^4$ yrs), carbon sequestration by weathering of continental rocks becomes an important process. Atmospheric CO_2 and H_2O reacts with rocks and is converted into aqueous bicarbonate that is transferred to the oceans via riverine discharge and eventually deposited on the seafloor as biogenic carbonates (Walker et al., 1981; Berner, 2004).
The hothouse climate during the PETM with an increase in precipitation and plant growth likely accelerated weathering. The associated large input of dissolved bicarbonates into the ocean would have neutralized the oceans' acidity and led to post-CIE deepening of the lysocline (Zachos et al., 2005), and preservation of calcareous marine sediments (Fig. 12; Kelly et al., 2010). This negative weathering feedback would ultimately have led to a draw-down of atmospheric CO_2, climatic cooling and reduced weathering.

6. Conclusive remarks

The PETM, represented by the largest perturbation in climate and carbon cyle during the last 60 million years (Fig. 1; Pearson & Palmer, 2000; Royer et al., 2007) can be considered as an analog for future climate change. The analysis of ice bubbles trapped in the Antarctic suggests a variability of the atmospheric CO_2 concentration over the last 800,000 yrs ranging from 172 ppmv to 300 ppmv for the preindustrial period. As a result of human activities, CO_2 in the atmosphere rose over the last couple of hundred years with a pace not seen in recent geological history. In the year 2011, the atmospheric CO_2 concentration exceeded 390 ppmv (Tans & Keeling, 2011), and a doubling of the pre-industrial atmospheric CO_2 level is expected by the end of this century. The climate sensitivity for this doubling in CO_2 is estimated to be 1.9–6.2 K due to the positive forcings, i.e. the rise in greenhouse gases, and including the negative forcing arising from the cooling effects of aerosols (IPCC, 2007; Andreae, 2007). A release of ~2000 PgC into the atmosphere in the next couple of hundred years could eventually trigger the release of an additional 2000-4000 PgC from marine sediments (Archer & Buffett, 2005), a flux comparable to that observed at the PETM (Zachos et al., 2008) and more than 10 times higher than observed during the last million years. The additional carbon release would act as a positive feedback, accelerating the warming.

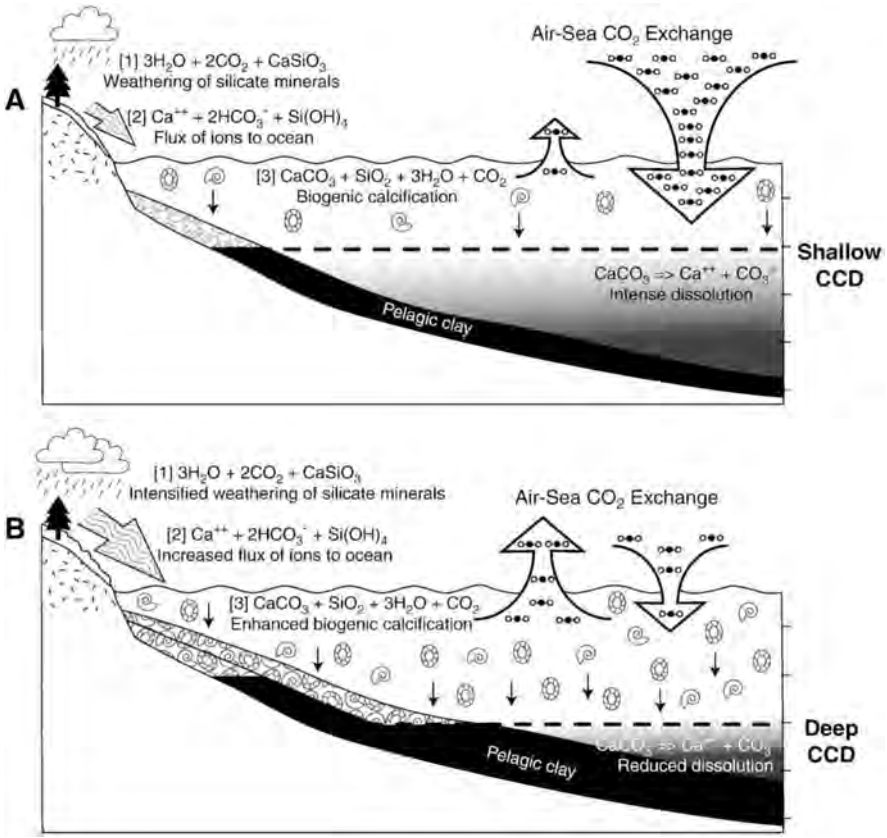

Fig. 12. Schematic changes in the carbonate–silicate geochemical cycle associated with the PETM (from Kelly et al., 2010). a) A rapid release of massive amounts of carbon into the ocean–atmosphere-biosphere system raises atmospheric pCO_2 levels, increases the carbon flux into the oceanic reservoir, thus raises the calcium carbonate compensation depth (CCD), and reduces the biogenic calcification. Preservation of carbonates is restricted to shallow areas on the seafloor. b) In the recovery phase of the atmosphere–ocean-biosphere system, silicate weathering is accelerated, reducing the atmospheric partial pressure of CO_2 and increasing the flux of dissolved bicarbonate ions and silicic acid to the ocean, thus neutralizing ocean acidification, and leading to a deepening of the CCD and preservation of carbonates in deeper areas on the seafloor. [Reproduced by permission of Elsevier; copyright 2010 Elsevier.]

The climatic and biogeochemical response to remarkable carbon emissions would likely be severe, for example a more frequent occurrence of climate extremes (heat waves, droughts and floods), particularly over the continents and at high latitudes, as well as ocean warming and stagnation. Another likely effect is ocean acidification and a rise of the calcite dissolution depth (Zachos et al., 2005), affecting marine organisms with calcareous shells (E. Thomas, 1998, 2003, 2007). The increased vertical gradients in the ocean together with warmer temperatures might produce near-anoxic conditions in the oxygen minimum zone

(comparable with dead zones in the Black Sea or the Gulf of Mexico). Geochemical evidence for the PETM supports a downward expansion of the oxygen-minimum zone below 1500 m (Chun et al., 2010; Nicolo et al., 2011) in agreement with foraminiferal evidence.

7. Acknowledgments

All model simulations were done on NCAR computers, supported by NSF. The work is supported by NSF Grant EAR-0628336.

8. References

Andreae, M.O., 2007: Atmospheric aerosols versus greenhouse gases in the twenty-first century. *Phil. Trans. R. Soc. London, A*, 365, 1915–1923. doi:10.1098/rsta.2007.2051.

Archer, D., & Buffett, B., 2005: Time-dependent response of the global ocean clathrate reservoir to climatic and anthropogenic forcing. *Geochemistry, Geophysics, Gesosystems,* 6, Q03002, doi:10.1029/2004GC000854.

Archer, D., Kheshgi, H., & Maier-Reimer, E., 1998: Dynamics of fossil fuel CO_2 neutralization by marine CaCO3. *Global Biogeochem. Cycles,* 12, 259–276.

Bains, S.R., Corfield, R., & Norris, R.D., 1999: Mechanisms of climate warming at the end of the Paleocene. *Science*, 285, 724–727, doi: 10.1126/science.285.5428.724.

Barron, E.J., Hay, W.W. & Thompson, S.,1989: The hydrologic cycle: a major variable during Earth history. *Palaeogeogr., Palaeoclimatol., Palaeoecol.,* 75, 157–174.

Beerling, D.J., Hewitt, C.N., Pyle, J.A., & Raven, J.A., 2007: Critical issues in trace gas biogeochemistry and global change. *Phil. Trans. R. Soc. London, A,* 365, 1629–1642.

Berner, R.A. (Ed.), 2004: The Phanerozoic Carbon Cycle: CO_2 and O_2, Oxford University Press, 150 pp.

Bice, K.L., & Marotzke, J., 2002: Could changing ocean circulation have destabilized methane hydrate at the Paleocene/Eocene boundary? *Paleoceanography*, 17, doi:10.1029/2001PA000678.

Bice, K.L., Scotese, C.R., Seidov, D., & Barron, E.J., 2000: Quantifying the role of geographic change in Cenozoic ocean heat transport using uncoupled atmosphere and ocean models. *Palaeogeogr,. Palaeoclimatol., Palaeoecol.,* 161, 295-310.

Boden, T.A., Marland, G., & Andres, R.J., 2010: Global, Regional, and National Fossil-Fuel CO_2 Emissions. Carbon Dioxide Information Analysis Center, Oak Ridge National Laboratory, U.S. Department of Energy, Oak Ridge, Tenn., U.S.A. doi: 10.3334/CDIAC/00001_V2010.

Bowen, G.J., & Bowen, B.B., 2008: Mechanisms of PETM global change constrained by a new record from central Utah. *Geology,* 36, 379-382.

Bowen, G.J., & Bowen, B.B., 2009: Mechanisms of PETM global change constrained by a new record from central Utah: Reply. *Geology,* 37, e185.

Bowen, G.J., & Zachos, J.C., 2010: Rapid carbon sequestration at termination of the Palaeocene-Eocene Thermal Maximum. *Nature Geoscience*, 3, 866-869, doi:10.1038/NGEO1014.

Bowen, G.J., Beerling, D.J., Koch, P.L., Zachos, J.C., & Quattlebaum, T., 2004: A humid climate state during the Paleocene/Eocene thermal maximum. *Nature,* 432, 495-499.

Bralower, T.J., Thomas, D.J. Zachos, J.C., Hirschmann, M.M., Röhl, U., Sigurdsson, H., Thomas, E., & Whitney, D.L., 1997: High-resolution records of the late Paleocene thermal maximum and circum-Caribbean volcanism: Is there a causal link? *Geology,* 25, 963-967.

Brinkhuis, H., et al., 2006: Episodic fresh surface waters in the Eocene Arctic Ocean. *Nature,* 441, 606-609.

Bujak, J.P., & Brinkhuis, H., 1998: Global warming and dinocyst changes across the Paleocene/Eocene epoch boundary. In: *Late Paleocene-early Eocene biotic and climatic events in the marine and terrestrial records*, Aubry, M.-P., Lucas, S., & Berggren, W.A. (Eds.), p. 277-295, Columbia University Press.

Burkholder, J.M., Noga, E.J., Hobbs, C.H., & Glascow, H.B., 1992: New phantom dinofagellate is the causative agent of major estuarine fish kills. *Nature*, 358, 407-410.

Caldeira, K., & Wickett, M.E., 2003: Anthropogenic CO_2 and ocean pH. *Nature*, 425, 365.

Charlson, R.J., Lovelock, J.E., Andreae, M.O. & Warren, S.G. 1987: Oceanic phytoplankton, atmospheric sulphur, cloud albedo and climate. *Nature,* 326, 661–665, doi:10.1038/326655a0.

Chun, C.O.J., Delaney, M.L., & Zachos, J.C., 2010: Paleoredox changes across the Paleocene-Eocene thermal maximum, Walvis Ridge (ODP Sites 1262, 1263, and 1266): Evidence from Mn and U enrichment factors. *Paleoceanography*, 25, doi:10.1029/2009PA001861.

Collins, W.D., et al., 2006: The Community Climate System Model Version 3 (CCSM3). *J. Climate,* 19, 2122-2143.

Cope, J.T., and Winguth, A., 2011: On the sensitivity of the Eocene ocean circulation to Arctic freshwater pulses. *Palaeogeogr., Palaeoclimatol., Palaeoecol.,* 306, 82–94.

Crouch, E.M., Heilmann-Clausen, C., Brinkhuis, H., Hugh E.G., Morgans, H.E.G., Rogers, K.M., Hans Egger, H., & Schmitz, B., 2001: Global dinoflagellate event associated with the late Paleocene thermal maximum. *Geology*, 29, 315-318, doi: 10.1130/0091-7613.

Cubasch, U., et al., 2001: Projections of future climate change. In: *Climate Change 2001: The Scientific Basis. Contribution of Working Group I to the Third Assessment report of the Intergovernmental Panel on Climate Change*, Houghton, J.T., Ding, Y., Griggs, D.J., Noguer, M., van der Linden, P.J., Dai, X., Maskell, K., & Voss, C.A. (Eds.), p. 525-582. Cambridge University Press, Cambridge, United Kingdom.

Cui, Y., Kump, L.R., Ridgwell, A.R., Charles, A.J., Junium, C.K., Diefendorf, A.F., Freeman, K.H., Urban, N.M. & Harding, I.C., 2011: Slow release of fossil carbon during the Palaeocene–Eocene Thermal Maximum, *Nature Geoscience,* 4, 481–485, doi: 10.1038/ngeo1179.

Dickens, G.R., & Quinby-Hunt, M.S., 1994: Methane hydrate stability in seawater. *Geophys. Res. Lett.*, 21, 2115-2118.

Dickens, G.R., O'Neil, J.R., Rea, D.K., & Owen, R.M., 1995: Dissociation of Oceanic Methane Hydrate as a Cause of the Carbon Isotope Excursion at the End of the Paleocene. *Paleoceanography,* 10, 965–971.

Dickens, G.R., Castillo, M.M., & Walker, J.C.G., 1997: A blast of gas in the latest Paleocene: Simulating first-order effects of massive dissociation of methane hydrate. *Geology,* 25, 259-262.

Fehsenfeld, F., et al., 1992: Emissions of volatile organic compounds from vegetation and their implications for atmospheric chemistry. *Global Biogeochem. Cycles,* 6, 389–430.

Gavrilov, Y., Shcherbinina, E.A., & Oberhänsli, H. 2003: Paleocene/Eocene boundary events in the northeastern Peri-Tethys. In: *Causes and Consequences of Globally Warm Climates in the Early Paleogene*, Wing, S.L., Gingerich, P.D., Schmitz, B., & Thomas, E. (Eds.), Geological Society of America, Special Paper, v. 369, p. 147-168.

Gleason, J.D., Thomas, D.J., Moore Jr., T.C., Blum, J.D., Owen, R.M., & Haley, B.A., 2009: Early to Middle Eocene History of the Arctic Ocean from Nd-Sr Isotopes in Fossil Fish Debris, Lomonosov Ridge. *Paleoceanography*, 24, PA2215, doi:10.1029/2008PA001685.

Guenther, A., Karl, T., Harley, P., Wiedinmyer, C., Palmer, P.I., & Geron, C. 2006: Estimates of global terrestrial isoprene emissions using MEGAN (model of emissions of gases and aerosols from nature). *Atmos. Chem. Phys. Discuss.*, 6, 107–173.

Handley, L., Pearson, P.N., McMillan, I.K., and Pancost, R.D., 2008: Large terrestrial and marine carbon and hydrogen isotope excursions in a new Paleocene/Eocene boundary section from Tanzania. *Earth Planet. Sci. Lett.,* 275, 17-25.

Handley, L., Crouch E.M., and Pancost R.D., 2011: A New Zealand record of sea level rise and environmental change during the Paleocene–Eocene Thermal Maximum. *Palaeogeogr., Palaeoclimatol., Palaeoecol*., 305, 185–200.

Head, J.J., Bloch, A.J., Hastings, I.K., Bourque, J.R., Cadena, E.A., Herrera, F.A., Polly, P.D. & Jaramillo, C.A., 2009: Giant boid snake from the Palaeocene neotropics reveals hotter past equatorial temperatures. *Nature,* 457, 715-717.

Heilmann-Clausen, C., & Egger, H., 2000: The Anthering outcrop (Austria): a key-section for correlation between Tethys and northwestern Europe near the Paleocene/Eocene boundary. *GFF*, 122, 69.

Heinemann, M., Jungclaus, J.H., & Marotzke, J., 2009: Warm Paleocene/Eocene Climate as simulated in ECHAM5/MPI-OM. *Climate of the Past Discussions*, 5, 1297-1336.

Higgins, J.A., & Schrag, D.P., 2006: Beyond methane: Towards a theory for Paleocene-Eocene Thermal Maximum. *Earth Planet. Sci. Lett.,* 245, 523-537.

Hollis, J.H., Handley, L., Crouch, E.M., Morgans, H.E.G., Baker, J.A., Creech, J., Collins, K.S., Gibbs, S.J., Huber, M., Schouten, S., Zachos, J.C., & Pancost, R.D., 2009: Tropical sea temperatures in the high-latitude South Pacific during the Eocene. *Geology,* 37, 99-102.

Houghton, R.A., 2008: Carbon Flux to the Atmosphere from Land-Use Changes: 1850-2005. In: *TRENDS: A Compendium of Data on Global Change*. Carbon Dioxide Information Analysis Center, Oak Ridge National Laboratory, U.S. Department of Energy, Oak Ridge, Tenn., U.S.A.

Huber, M., & Sloan, L.C., 1999: Warm climate transitions: A general circulation modeling study of the Late Paleocene Thermal Maximum. *J. Geophys. Res.,* 104, 16633-16655.

Huber, M., & Sloan, L.C., 2001: Heat transport, deep waters, and thermal gradients: Coupled simulation of an Eocene greenhouse climate. *Geophys. Res. Lett.,* 28, 3481-3484.

Huber, M., & Caballero, R., 2003: Eocene El Niño: Evidence for robust tropical dynamics in the "hothouse". *Science,* 299, 877-881.

Huber, M., & Caballero, R., 2011: The early Eocene equable climate problem revisited. *Clim. Past*, 7, 603-633doi:10.5194/cp-7-603-2011.

Iakokleva, A.I., Brinkhuis, H., & Cavagnetto, C., 2001: Late Paleocene-Early Eocene dinoflagellae cysts from the Turgay Strait, Kazakhstan; correlations across ancient seaways. *Paleogeogr., Paleoclimatol., Paleoecol.,* 172, 243-268.

IPCC, 1990: *Report prepared for Intergovernmental Panel on Climate Change by Working Group I.* Houghton, J.T., Jenkins G.J. & Ephraums J.J. (Eds.), Cambridge University Press, Cambridge, Great Britain, New York, NY, USA and Melbourne, Australia, 410 pp.

IPCC, 2007: *Climate Change 2007: The Physical Science Basis. Contribution of Working Group I to the Fourth Assessment Report of the Intergovernmental Panel on Climate Change*. Solomon, S., Qin, D., Manning, M., Chen, Z., Marquis, M., Averyt, K.B., Tignor, M., & H.L. Miller (Eds.), Cambridge University Press, Cambridge, United Kingdom and New York, NY, USA, 996 pp.

Kelly, D.C., Bralower, T.J. & Zachos, J.C. 1998: Evolutionary consequences of the latest Paleocene Thermal Maximum for tropical planktonic foraminifera. *Paleogeogr., Paleoclimatol., Paleoecol.,* 141, 139-161.

Kelly, D.C., Nielsen, T.M.J., McCarren, H.K., Zachos, J.C., & Röhl, U., 2010: Spatiotemporal patterns of carbonate sedimentation in the South Atlantic: Implications for carbon cycling during the Paleocene–Eocene thermal maximum. *Paleogeogr., Paleoclimatol., Paleoecol.,* 293, 30-40.

Kennett, J.P., & Stott, L.D., 1991: Abrupt deep-sea warming, paleoceanographic changes and benthic extinctions at the end of the Paleocene. *Nature,* 353, 225-229.

Kirk-Davidoff, B.D., Schrag, D.P., & Anderson, J.G., 2002: On the feedback of stratospheric clouds on polar climate. *Geophys. Res. Lett.,* 29, 1556, doi:10.1029/2002GL014659.

Koch, P.L., Zachos, J.C., & Gingerich, P.D., 1992: Correlation between isotope records in marine and continental carbon reservoirs near the Palaeocene/Eocene boundary. *Nature,* 358, 319-322.

Korty, R.L., Emanuel, K.A., & Scott, J.R., 2008: Tropical cyclone-induced upper ocean mixing and climate: application to equable climates. *J. Climate,* 21, 638-654.

Kump, L.R., & Pollard, D., 2008: Amplification of Cretaceous warmth by biological cloud feedbacks. *Science*, 320, 195.

Lu, G., Keller, G. & Pardo, A., l998: Stability and change in Tethyan planktic foraminifera across the Paleocene-Eocene transition. *Mar. Micropaleontol.,* 35, 203-233.

Lunt, D.J., Valdes, P.J., Jones, T.D., Ridgwell, A., Haywood, A.M., Schmidt, D.N., Marsh, R., & Maslin, M., 2010: CO_2-driven ocean circulation changes as an amplifier of Paleocene-Eocene thermal maximum hydrate destabilization. *Geology*, 38, 875-878, doi: 10.1130/G31184.1.

Lyle, M., Barron, J., Bralower, T.J., Huber, M., Olivarez Lyle, A., Ravelo, A.C., Rea, D.K., & Wilson, P.A., 2008: Pacific Ocean and Cenozoic evolution of climate. *Rev. Geophys.,* 46, 1-47.

Maclennan, J., & Jones, S.M., 2006: Regional uplift, gas hydrate dissociation and the origins of the Paleocene-Eocene Thermal Maximum. *Earth Planet. Sci. Lett.,* 245, 65-80.

Marincovich, L., Jr., & Gladenkov, A.Y., 1999: Evidence for an early opening of the Bering Strait. *Nature,* 397, 149–151.

Meehl, G.A., Washington, W.M., Santer, B.D., Collins, W.D., Arblaster, J.M., Hu, A., Lawrence, D.M., Teng, H. Buja, L.E. & Strand, W.G., 2006: Climate change projections for the twenty-first century and climate change commitment in the CCSM3. *J. Climate,* 19, 2597-2616.

Mikolajewicz, U., Gröger, M., Maier-Reimer, E., Schurgers, G., Vizcaíno, M., & Winguth, A., 2007: Long-term effects of anthropogenic CO_2 emissions simulated with a complex earth system model. *Clim. Dyn.*, 28, 599-633.

Moran, K., et al., 2006: The Cenozoic palaeoenvironment of the Arctic Ocean. *Nature,* 441, 601-605.

Nicolo, M.J., Dickens, G.R., & Hollis, C.J., 2011: South Pacific intermediate water oxygen depletion at the onset of the Paleocene-Eocene Thermal Maximum as depicted in New Zealand margin sections. *Paleoceanography*, in press.

Nunes, F., & Norris, R.D. 2006: Abrupt reversal in ocean overturning during the Paleocene/Eocene warm period. *Nature,* 439, 60-63.

Pagani, M., Pedentchouk, N. Huber, M., Sluijs, A., Schouten, S., Brinkhuis, H., Sinninghe, J.S., Damsté, Dickens, G.R., & the Expedition 302 Scientists, 2006a: Arctic hydrology during global warming at the Paleocene/Eocene thermal maximum. *Nature,* 442, 671-675.

Pagani, M., Caldeira, K., Archer, D., & Zachos, J.C., 2006b: An ancient carbon mystery. *Science,* 314, 1556-1557.

Panchuk, K., Ridgwell, A. & Kump, L.R., 2008: The sedimentary response to Paleocene-Eocene Thermal Maximum carbon release: A model-data comparison. *Geology,* 36, 315-318.

Pancost, R.D., Steart, D.S., Handley, L., Collinson, M.E., Hooker, J.J., Scott, A.C., Grassineau, N.V., & Glasspool, I.J., 2007: Increased terrestrial methane cycling at the Palaeocene-Eocene thermal maximum. *Nature,* 449, 332-335.

Pearson, P.N., & Palmer, M.R. 2000: Atmospheric carbon dioxide concentrations over the past 60 million years. *Nature,* 406, 695-699.

Pearson, P.N., van Dongen, B.E., Nicholas, C.J., Pancost, R.D., Schouten, S., Singano, J.M., & Wade, B.S., 2007: Stable warm tropical climate through the Eocene Epoch. *Geology,* 35, 211-214.

Prather, M., & Ehhalt, D., 2001: Atmospheric chemistry and greenhouse gases. In: *Climate change 2001. The scientific basis*, Houghton, J.T., Ding, Y., Griggs, D.J., Noguer, M., van der Linden, P.J., Dai, X., Maskell, K., & Johnson, C.A. (Eds.), p. 239–287. Cambridge, UK: Cambridge University Press.

Ravizza, G., Norris, R.N., Blusztajn, J., & Aubry, M.-P., 2001: An osmium isotope excursion associated with the late Paleocene thermal maximum: Evidence of intensified chemical weathering. *Paleoceanography*, 16, 155-163.

Retallack, G.J., 2005: Pedogenic carbonate proxies for amount and seasonality of precipitation in paleosols. *Geology,* 33, 333-336.

Retallack, G.J., 2009: Mechanisms of PETM global change constrained by a new record from central Utah: Comment. *Geology,* 37, e184-e185.

Robert, C., & Kennett, J.P., 1994: Antarctic subtropical humid episode at the Paleocene-Eocene boundary: Clay-mineral evidence. *Geology,* 22, 211-214.

Roberts, C.D., LeGrande, A.N., & Tripati, A.K., 2009. Climate sensitivity to Arctic seaway restriction during the Early Paleogene. *Earth and Planetary Science Letters*, 286, 576-585.

Royer, D.L., Berner, R.A., & Park, J., 2007: Climate sensitivity constrained by CO_2 concentrations over the past 420 million years. *Nature,* 446, 530-532.

Schmidt, G.A., & Shindell, D.T., 2003: Atmospheric composition, radiative forcing, and climate change as a consequence of a massive methane release from gas hydrates. *Paleoceanography*, 18, 1004, doi:10.1029/2002PA000757.

Schmitz, B., & Pujalte, V., 2007: Abrupt increase in seasonal extreme precipitation at the Paleocene-Eocene boundary. *Geology,* 35, 215-218.

Schmitz, B., Speijer, R.P., & Aubry, M.P., 1996: Latest Paleocene benthic extinction event on the southern Tethyan shelf (Egypt): Foraminiferal stable isotopic ($\delta^{13}C$, $\delta^{18}O$) records. *Geology,* 24, 347-350.

Scotese, C.R., 2011: PALEOMAP, date of access: 07/05/2011, available from: <http://www.scotese.com>.

Sewall, J. O., & Sloan, L.C. 2006: Come a little bit closer: A high-resolution climate study of the early Paleogene Laramide foreland. *Geology,* 34, 81-84.

Shellito C.J., & Sloan, L.C., 2006: Reconstructing a lost Eocene paradise: Part I. Simulating the change in global floral distribution at the initial Eocene thermal maximum. *Global Planet. Ch.,* 50, 1-17.

Shellito, C.J., Sloan, L.C., & Huber, M., 2003: Climate model sensitivity to atmospheric CO_2 levels in the Early-Middle Paleogene. *Paleogeogr., Paleoclimatol., Paleoecol.,* 193, 113-123.

Shellito, C.J., Lamarque, J.-F. & Sloan, L.C., 2009: Early Eocene Arctic climate sensitivity to pCO_2 and basin geography. *Geophys. Res. Lett.,* 36, L09707, doi:10.1029/ 2009GL037248.

Sloan, L.C. & Barron, E.J., 1992: Eocene climate model results: Quantitative comparison to paleo-climatic evidence. *Palaeogeogr., Palaeoclim., Palaeoecol.,* 93, 183-202.

Sloan, L.C., & Pollard, D., 1998: Polar stratospheric clouds: A high latitude warming mechanism in an ancient greenhouse world. *Geophys. Res. Lett.*, 25, 3517–3520.

Sloan, L.C., & Rea, D.K., 1995: Atmospheric carbon dioxide and early Eocene climate: A general circulation modeling sensitivity study. *Palaeogeogr., Palaeoclim., Palaeoecol.,* 119, 275-292.

Sluijs, A., 14 others, & the Expedition 302 Scientists, 2006: Subtropical Arctic Ocean temperatures during the Paleocene/Eocene thermal maximum. *Nature,* 441, 610-613.

Sluijs, A., Brinkhuis, H., Schouten, S., Bohaty, S.M., John, C.M., Zachos, J.C., Reichart, G.-J., Sinninghe Damsté, J.S., Crouch, E.M., & Dickens, G.R., 2007: Environmental precursors to rapid light carbon injection at the Palaeocene/Eocene boundary. *Nature,* 450, 1218-1221.

Sluijs, A., Röhl, U., Schouten, S., Brumsack, H.-J., Sangiorgi, F., Sinninghe Damsté, J.S., & Brinkhuis, H., 2008a: Arctic Late Paleocene – Early Eocene paleoenvironments with special emphasis on the Paleocene – Eocene thermal maximum (Lomonosov Ridge, IODP Expedition 302). *Paleoceanography,* 23, PA1S11, doi:10.1029/2007PA001495.

Sluijs, A., et al., 2008b: Eustatic variations during the Paleocene-Eocene greenhouse world. *Paleoceanography,* 23, PA4216, doi:10.1029/2008PA001615.

Sluijs, A. Bijl, P.K., Schouten, S., Roehl, U., Reichart, G.-J., and Brinkhuis, H., 2011: Southern ocean warming, sea level and hydrological change during the Paleocene-Eocene thermal maximum. *Climate of the Past*, 7, 47–61.

Speijer, R.P., & Wagner, T., 2002: Sea-level changes and black shales associated with the late Paleocene Thermal Maximum (LPTM): Organic geochemical and

micropaleontologic evidence from the southern Tethyan margin (Egypt-Israel). In: *Catastrophic events and mass extinctions*: Impacts and beyond, Koeberl, C., and MacLeod, K.G. (Eds.), Geological Society of America Special Paper, 356, p. 533–549.

Stoll, H.M., Shimizu, N., Ziveri, P., & Archer, D., 2007: Coccolithophore productivity response to greenhouse event of the Paleocene-Eocene Thermal Maximum. *Earth and Planetary Science Letters*, 258, 192-206.

Storey, M., Duncan, R.A., & Swisher III, C.C., 2007: Paleocene-Eocene Thermal Maximum and the opening of the Northeast Atlantic. *Science,* 316, 587-589.

Svensen, H., Planke, S., Malthe-Sørenssen, A., Jamtveit, B., Myklebust, R., Eidem, T.R., & Rey, S.S., 2004: Release of methane from a volcanic basin as a mechanism for initial Eocene global warming. *Nature,* 429, 542-545.

Tans, P., & Keeling, R., 2011: Trends in atmospheric carbon dioxide., *NOAA/ESRL and Scripps Institution of Oceanography,* date of access: 07/05/2011, available from: <http://www.esrl.noaa.gov/gmd/ccgg/trends/>

Thomas, D.J., 2004: Evidence for deep-water production in the North Pacific Ocean during the early Cenozoic warm interval. *Nature*, 430, 65-68.

Thomas, D.J., Lyle, M., Moore, T.C., Jr., & Rea, D.K., 2008: Paleogene deep-water mass composition of the tropical Pacific and implications for thermohaline circulation in a Greenhouse World. *Geochemistry, Geophysics, Geosystems*, 9, 1-13, doi:10.1029/ 2007GC001748.

Thomas, E., 1998: The biogeography of the late Paleocene benthic foraminiferal extinction, In: *Late Paleocene-early Eocene biotic and climatic events in the marine and terrestrial records*, Aubry, M.-P., Lucas, S., & Berggren, W.A. (Eds.), , p. 214-243, Columbia University Press.

Thomas, E., 2003: Extinction and food at the seafloor: A high-resolution benthic foraminiferal record across the initial Eocene Thermal Maximum, Southern Ocean Site 690. *GSA Spec. Paper,* 369, 319-332.

Thomas, E., 2007: Cenozoic mass extinctions in the deep sea; what disturbs the largest habitat on Earth? In: *Large Ecosystem Perturbations: Causes and Consequences:* Monechi, S., Coccioni, R., & Rampino, M. (Eds.), *GSA Special Paper*, 424, 1-24.

Thomas, E., Zachos, J.C., & Bralower, T. J., 2000: Deep-Sea Environments on a Warm Earth: latest Paleocene - early Eocene. In: *Warm Climates in Earth History*, Huber, B., MacLeod, K., and Wing, S. (Eds.), pp. 132-160, Cambridge University Press, Cambridge, United Kingdom.

Tripati, A., & Elderfield, H. 2005: Deep-sea temperature and circulation changes at the Paleocene-Eocene Thermal Maximum. *Science,* 308, 1894-1898.

Walker, J.C.G., Hays, P.B., & Kasting, J.F., 1981: A negative feedback mechanism for thelong-term stabilization of earth's surface temperature. *Journal of Geophysical Research,* 86 (C10), 9776–9782.

Weijers, J.W.H., Schouten, S., Sluijs, A., Brinkhuis, H., & Sinninghe Damsté, J.S., 2007: Warm arctic continents during the Paleocene-Eocene thermal maximum. *Earth Planet. Sci. Lett.,* 261, 230-238.

Wing, S.L., Harrington, G.J., Smith, F.A., Bloch, J.I., Boyer, D.M., & Freeman, K.H., 2005: Transient floral change and rapid global warming at the Paleocene-Eocene boundary. *Science,* 310, 993-996.

Winguth, A.M.E., Shellito, C., Shields, C., & Winguth, C., 2010: Climate response at the Paleocene-Eocene Thermal Maximum to greenhouse gas forcing – A model study with CCSM3. *J. Climate*, 23, 2562-2584, doi:10.1175/2009JCLI3113.1.

Zachos, J.C., & Dickens, G.R., 2000: An assessment of the biogeochemical feedback response to the climatic and chemical perturbations of the LPTM. *Gff*, 122, 188-189.

Zachos, J.C., et al., 2005: Rapid acidification of the ocean during the Paeocene-Eocene thermal maximum. *Science,* 308, 1611-1615.

Zachos, J.C., Bohaty, S.M., John, C.M., McCarren, H., Kelly, D.C., & Nielsen, T., 2007: The Paleocene-Eocene carbon isotope excursion: constraints from individual shell planktonic foraminifer records. *Phil. Trans. R. Soc. London, A,* 365, 1829-1842.

Zachos, J.C., Dickens, G.R., & Zeebe, R.E., 2008: An early Cenozoic perspective on greenhouse warming and carbon cycle dynamics. *Nature,* 451, 279-283.

Zeebe, R.E., & Zachos, J.C., 2007: Reversed Deep-Sea Carbonate Ion Basin Gradient During Paleocene-Eocene Thermal Maximum. *Paleoceanography*, 22, PA3201, doi:1029/ 2006PA001395.

Zeebe, R.E., Zachos, J.C., & Dickens, G.R., 2009: Carbon dioxide forcing alone insufficient to explain Palaeocene-Eocene Thermal Maximum warming. *Nature Geoscience*, 2, 576-580.